ELSEVIER

Full paper/Mémoire

Comparative assessment of the ability of a microwave absorber nanocatalyst in the microwave-assisted biodiesel production process

Hamed Nayebzadeh [a, c, *], Naser Saghatoleslami [a], Mohammad Haghighi [b, c], Mohammad Tabasizadeh [d], Ehsan Binaeian [e]

[a] *Department of Chemical Engineering, Faculty of Engineering, Ferdowsi University of Mashhad, P.O. Box 9177948974, Mashhad, Iran*
[b] *Chemical Engineering Faculty, Sahand University of Technology, P.O. Box 51335-1996, Sahand New Town, Tabriz, Iran*
[c] *Reactor and Catalysis Research Center (RCRC), Sahand University of Technology, P.O. Box 51335-1996, Sahand New Town, Tabriz, Iran*
[d] *Department of Biosystems Engineering, Faculty of Agriculture, Ferdowsi University of Mashhad, P.O. Box 9177948974, Mashhad, Iran*
[e] *Department of Chemical Engineering, Qaemshahr Branch, Islamic Azad University, Qaemshahr, Iran*

A B S T R A C T

In this study, a carbon-supported $KOH/Ca_{12}Al_{14}O_{33}$ nanocomposite was fabricated via the microwave combustion method, in which dextrose was used as a carbon source, and its activity in the microwave-assisted transesterification reaction as a microwave absorption material was assessed. The samples were characterized by X-ray diffraction, Fourier transform infrared spectroscopy, thermogravimetry, Brunauer−Emmett−Teller (BET), field-emission scanning electron microscopy, and energy dispersive X-ray analyses. The results showed that the carbonate and noncarbonate samples had a calcium aluminate ($Ca_{12}Al_{14}O_{33}$) structure as a support. Different carbon groups were formed during preparation of the carbon-supported $KOH/Ca_{12}Al_{14}O_{33}$ nanocomposite, which improved its surface area and porosity. Although the samples presented similar basicity, the carbonated nanocomposite exhibited twice as much activity as the $KOH/Ca_{12}Al_{14}O_{33}$ nanocatalyst for conversion of canola oil to biodiesel in the microwave-assisted transesterification reaction at 270 W microwave power. The nanocomposite with a larger pore size made active sites easily accessible and exhibited higher catalytic ability where the conversion of 98.8% was obtained under the optimized conditions of 270 W microwave power, methanol/oil molar ratio of 15, 4 wt% of the nanocomposite, and 30 min of reaction time. The carbon-supported nanocatalyst can be reused for at least four times with less reduction in activity. Furthermore, the obtained biodiesel showed that it met the standard values (EN 14214 and ASTM D-6751) with respect to the density, kinematic viscosity at 40 °C, acid number, and flash point.

© 2018 Académie des sciences. Published by Elsevier Masson SAS. All rights reserved.

1. Introduction

Nowadays, researchers attempt to accelerate the reaction to reduce the requirement time for obtaining products.

Therefore, the conventional heating systems were replaced by new technologies such as microwave, ultrasonic, and super/subcritical processes. The microwave heating technique has been successfully used in various chemical processes such as nanomaterial synthesis, solid-state chemistry, nanotechnology, and organic chemistry. Microwave irradiation rapidly and homogeneously increases the temperature of a reaction medium such that the higher reaction rate and selectivity of the ensuring products can be

obtained by choosing appropriate microwave parameters [1,2].

Biodiesel production is one of the chemical reactions that can be performed by microwave irradiation, in which the reaction and separation times are reduced significantly from hours to minutes. Biodiesel is commonly produced by transesterification of edible and nonedible oils in the presence of short chain alcohol, where methanol is usually used because of its high activity and low price, using a catalyst. To further increase the compatibility of the biodiesel production process with the environment, heterogeneous catalysts are suggested instead of homogeneous catalysts [3,4]. Some heterogeneous catalysts such as CaO [5–7], $NaOCH_3$ [8], $NaNH_2$ [9], heteropolyacid catalyst [10,11], and sulfated zirconia [12] have been examined in the microwave-assisted transesterification reaction (MTR). In addition to strong stability and less leaching of active phases of catalysts in the reaction mixture, high specific surface area, strong base strength, and high concentration of base sites are characteristics of an active transesterification catalyst [13].

Alkaline earth aluminates with formula $M_xAl_{2y}O_{x+3y}$ (M = Ca, Mg, Sr, and Ba) as active and stable support may be an appropriate choice for use in the biodiesel production because it can be easily synthesized via the microwave combustion method (MCM) with a high surface area in very short time. The activity of a $MgO/MgAl_2O_4$ nanocatalyst synthesized by the combustion method was studied in the biodiesel production and yield of 95.7% was obtained under the conditions of 110 °C, methanol/oil molar ratio of 12, 3 wt% of the catalyst, and reaction time of 3 h [14]. The CaO/$Ca_{12}Al_{14}O_{33}$ catalyst also converted 98.7% of vegetable oil to the biodiesel at 65 °C, 1:10 oil/methanol ratio, and 6 wt% of the catalyst for 3.5 h [15]. The $KF/Ca_xAl_2O_{(x+3)}$ catalyst was evaluated to catalyze the transesterification reaction of soybean oil with methanol [16]. The yield of 98% was obtained under the conditions of 60 °C, methanol/oil molar ratio of 18, 3 wt% of the catalyst, and 5 h of reaction time when the catalyst showed less stability. In our previous work, KOH/calcium aluminate was successfully synthesized by the MCM and showed high activity in the transesterification reaction of canola oil [17]. However, no study has so far been done on the activity of these catalysts in the MTR.

It is well known that using microwave absorbing materials is important for further accelerating the reaction rate. If the catalyst is a strong microwave absorber material, it can gather the microwave irradiation and the "microwave hot spots" would be consequently formed [18]. Therefore, carbonated catalysts can have an opportunity to achieve the highest reaction rate, which have been examined in a few studies for biodiesel production via the esterification reaction [18,19]. However, according to the best of best knowledge, carbonated alkaline earth aluminate catalyst prepared via a simple MCM has not been used for biodiesel production via the MTR.

The triple objectives of this study were as follows: first, to develop an experimental procedure for preparation of a KOH-containing $Ca_{12}Al_{14}O_{33}$/C nanocomposite as a high active microwave absorbing material via the simple MCM; second, to evaluate the influence of absorbed microwave energy on the rate of transesterification reaction; and third, to obtain a sample with high stability in the MTR for industrial application. The samples (carbonated and noncarbonated) were characterized by X-ray diffraction (XRD), Fourier transform infrared spectroscopy (FTIR), thermogravimetry (TG), BET–Barrett-Joyner-Halenda (BJH), field-emission scanning electron microscopy (FESEM), and energy dispersive X-ray (EDX) analyses, and their basicity was evaluated by the Hammett indicator method. Finally, the MTR parameters were optimized.

2. Materials and methods

2.1. Catalyst preparation

$Ca_{12}Al_{14}O_{33}$ (CA) was prepared by the MCM using urea as fuel with stoichiometric compositions, according to the concepts of propellant chemistry. For this purpose, 12 mmol $Ca(NO_3)_2 \cdot 4H_2O$, 14 mmol $Al(NO_3)_3 \cdot 9H_2O$, and 55 mmol urea were dissolved in 40 mL distilled water and the mixture was heated on the hotplate at 80 °C under stirring to form viscous gel. Then, the mixture was placed in the microwave oven (Daewoo, Model No. KOC9N2TB, 900 W, 2.45 GHz) and irradiated for 10 min. After evaporation of remained water and exhaustion of the gases, the mixture was flamed for a few seconds and fumy white powder was synthesized. The CA/C nanocomposite was synthesized as described above where dextrose (13.75 mmol) was used instead of urea. Finally, the brown powder was prepared when no flame was observed.

Finally, the samples were impregnated by the KOH where 1 g of each sample was mixed with 35.6 mL of a 0.1 M KOH aqueous solution and heated at 80 °C to form gel. After drying at 110 °C overnight, the solution was calcined at 800 °C for 3 h under argon medium. The samples were labeled as KCA and KCA/C. The catalyst preparation routes are shown in Fig. S1 of the Supplementary Material (SM).

2.2. Catalyst characterization

The crystalline phase of the samples was detected by XRD analysis using a Unisantis XMD 300 by means of Cu Kα radiation operating at 45 kV and 80 mA with scanning range of 10–70°. The active surface functional groups of the synthesized nanocomposites were evaluated by the FTIR in the range of 400–4000 cm^{-1} using a Shimadzu 4300 (Japan) spectrometer. The decomposition of raw materials and fuels during catalyst preparation was analyzed by thermogravimetry analysis (TGA). The TGA was performed using an evolution STA (SETARAm, France) instrument in the range of 50–800 °C at a heating rate of 20 °C/min under the airflow. The specific surface area, mean pore size, and pore volume of the nanocomposites were assayed using a PHS-1020 (Phschina, China) apparatus by the BET–BJH methods. FESEM analysis was accomplished to study the morphology and surface structure of the nanocomposites using MIRA3 FEG-SEM (TESCAN, Czech Republic). The distribution of elements in the samples was quantified by EDX technique using a VEGA II detector (TESCAN). The basic strength of the solid bases (H_) was determined by using Hammett indicators. The indicators used were as follows:

bromothymol blue (H_ = 7.2), phenolphthalein (H_ = 9.8), and 2,4-dinitroaniline (H_ = 15.0). To measure the basicity of the nanocatalysts, the method of Hammett indicator −benzene carboxylic acid (0.02 mol/L anhydrous ethanol solution) titration was used [20].

2.3. Microwave-assisted transesterification reaction

The activity of the samples was assessed in the MTR, in which 20 g canola oil (acid value, 0.05%; molecular weight, 850 g.gmol^{-1}), 17 mL methanol (18 methanol/oil molar ratio), and 0.8 g catalyst (4 wt %) were poured in a 100 mL glass reactor equipped with a water-cooled condenser. The MTR was performed in a domestic microwave oven at different microwave output powers (180, 270, 360, 450, and 540 W) for 45 min. After the reaction, the mixture was centrifuged at 2500 rpm for 25 min (Chemical Sahand Co., Iran) and the upper liquid phase (containing biodiesel) was separated. Finally, the layer was heated to remove excess methanol and analyzed by gas chromatography (GC, Teif Gostar Faraz Co., Iran) equipped with flame ionization detector (FID) and Select Biodiesel CP9080 capillary column (30 m × 0.32 mm × 0.25 μm) to obtain the fatty acid methyl ester (FAME) content as in the following reaction.

In each run, the 0.5 μL sample containing 100 μL of biodiesel was dissolved in 1 mL of n-hexane and 1 μL of an internal standard solution (nonadecanoic acid methyl ester) was injected into the GC at a temperature of 60 °C. After holding for 2 min, the GC oven was heated at 10 °C/min rate to 210 °C. Then, it was heated at 5 °C/min rate to 230 °C and held for 10 min. Hydrogen was a carrier gas. The injector and FID were set up to an operating temperature of 250 °C. Helium gas was used as carrier gas with a flow rate of 1 mL/min.

3. Results and discussion

3.1. XRD analysis

The XRD patterns of the samples are illustrated in Fig. 1. It is well known that the type of fuel can significantly affect
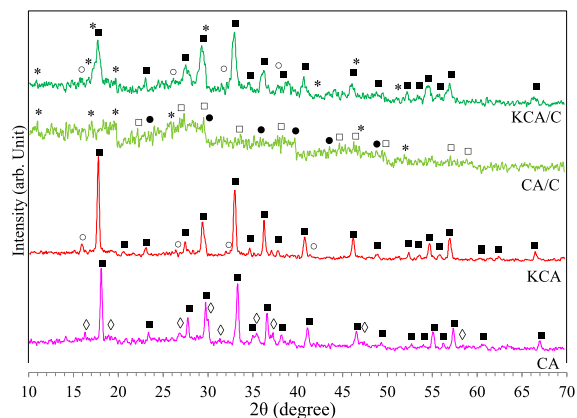
Fig. 1. The XRD plots of (a) calcium aluminate, (b) KOH/calcium aluminate and carbonated (c) calcium aluminate and (d) KOH/calcium aluminate nanocatalysts. (■) $Ca_{12}Al_{14}O_{33}$, (◇) $CaAl_2O_4$, (□) $Ca_3Al_2O_6$, (●) $CaCO_3$, (○) K_3AlO_3, and (*) C.

the properties of synthesized powder using the MCM due to the different temperature of the combustion reaction. It was reported that the reaction between CaO and Al_2O_3 resulted in the formation of $Ca_3Al_2O_6$, $Ca_{12}Al_{14}O_{33}$, $CaAl_2O_4$, $Ca_5Al_6O_{14}$, $CaAl_4O_7$, $CaAl_{12}O_{19}$, and Al_2O_3, subsequently. Formation of each of these structures depends on the temperature of the combustion reaction. Fig. 1a shows the $Ca_{12}Al_{14}O_{33}$ (JCPDS No. 70-2144) and $CaAl_2O_4$ (JCPDS No. 70-0134) structures formed due to a high temperature of the combustion reaction using urea. However, the powder synthesized by dextrose (Fig. 1c) showed amorphous structure with some diffraction peaks of $Ca_3Al_6O_{14}$ (JCPDS No. 33-0251), $CaCO_3$ (formed by the reaction between CaO and CO_2 in the air, JCPDS No. 72-1937), and carbon (JCPDS No. 18-0311). According to Fig. 1b, CA was completely transformed to mayenite structure with calcination. Moreover, the K_3AlO_3 phase (JCPDS No. 27-1336) was detected to be able to increase its activity. These structures were formed by a reaction between K_2O and Al_2O_3 at a high calcination temperature [21]. The KCA/C nanocomposite showed that the mayenite structure ($Ca_{12}Al_{14}O_{33}$, JCPDS No. 48-1882) was different from that of the KCA sample, and K_3AlO_3 and carbon were also formed after calcination (see Fig. 1d). Some other peaks were seen to be related to the carbon groups. Furthermore, some peaks of potassium linked to carbon were also detected. Formation of carbon can significantly increase the ability of a catalyst to absorb the microwave irradiation.

3.2. Thermogravimetry analysis

TGA of the samples under atmosphere medium are illustrated in Fig. 2 where the CA/C and KCA/C catalysts showed higher weight loss that can be assigned to the carbon groups existing in these samples. The CA catalyst showed three weight losses: first, 2.13% loss of weight between 25 and 120 °C corresponding to physically absorbed water; second, 10.2% weight loss in the range of 150−475 °C mainly due to the loss of structural water and pyrolysis of organic groups (unreacted urea or nitrate components) [22,23]; and third, the last weight loss (4%) occurring between 474 and 565 °C, which was related to the diffusion of
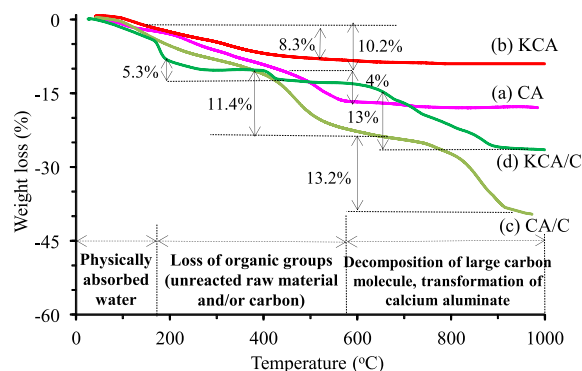
Fig. 2. TGA plots of (a) calcium aluminate, (b) KOH/calcium aluminate and carbonated (c) calcium aluminate and (d) KOH/calcium aluminate nanocatalysts.

Ca ions in calcium aluminate lattice. A little reduction in weight can be detected around 700 °C, which can be attributed to the transformation of calcium aluminate phases from $CaAl_2O_4$ to $Ca_{12}Al_{14}O_{33}$. The CA/C sample showed a similar behavior with CA until 730 °C, whereas the loss of weight was higher than that in CA, which could correspond to the oxidation of the carbon groups [24]. However, the last weight loss (13.2%) can be assigned to the arrangement of calcium aluminate structure and decomposition of carbon groups with a large structure, as supported by the XRD results [25].

The KCA sample showed the lowest weight loss (8.3%) corresponding to dehydroxylation of the OH units, which highlighted its high crystallinity and well perching of potassium components to the surface of a support. The KCA/C sample showed three weight losses that were, respectively, related to the loss of adsorbed water (7.8%), decomposition of the carbon structure with low molecular weight (5.3%), and decomposition of a large molecule of carbon components (13%) [26]. It must be noted that transformation of a few remained calcium aluminates to the mayenite structure was carried out over the same temperature range, but these processes were hindered by the carbon oxidation. Moreover, the results of the thermal analysis suggested that the proper calcination temperature of the solid base catalyst was in the range of 700–900 °C (according to the CA/C TG plot), which authenticated the appropriateness of calcination temperature, as was selected in this study (800 °C).

3.3. FTIR analysis

FTIR spectra of the KCA and KCA/C nanocomposites are illustrated in Fig. 3. The KCA nanocatalyst showed four sharp peaks at 460, 570, 845, and 1410 cm^{-1} corresponding to vibration of Ca–O, Al–O (in AlO_6), Al–O (in AlO_4), and Ca/Al–O-X (X = H or K), respectively [4,27]. Moreover, a broad bond at 2800–3600 cm^{-1} was assigned to vibration of the O–H bond related to absorbed water on the surface of the sample and/or the Ca/Al–OH groups. It has been reported that interaction between potassium (hydrogen) components and support components (Ca and Al) can be
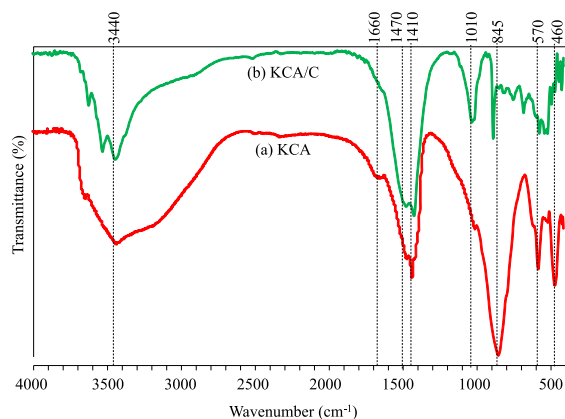

Fig. 3. FTIR spectra of (a) KOH/$Ca_{12}Al_{14}O_{33}$ and (b) carbonated KOH/$Ca_{12}Al_{14}O_{33}$ nanocatalysts.

observed above 3500 cm^{-1} [28]. The bending vibration of the O–H groups was observed at 1660 cm^{-1} [14].

The KCA/C nanocomposite showed different peaks below 1100 cm^{-1} and above 3200 cm^{-1}. The stretching vibration of C–C can be seen at 1010 cm^{-1} [29,30]. The Al–O bonds were not sharp like the KCA nanocatalyst, which can be due to the formation of other bonds with low polarity that reduced the intensity of the Al–O bonds. Many peaks can be observed in the region of 500–900 cm^{-1} corresponding to the C–K groups as described in the XRD pattern [31]. The carbon groups covered all crystals and affected vibration of these bonds. It should be noted that the carbon–carbon bonds can be detected below 1000 cm^{-1}, which could indicate the presence of the carbon-heavy groups [32]. The KCA/C nanocomposite also showed low hydrophilic property as compared to KCA, where the bending vibration of the O–H group was not observed at 1660 cm^{-1}.

3.4. FESEM and EDX analysis

The FESEM images of the KCA and KCA/C nanocomposites are shown in Fig. 4. The KCA nanocatalyst showed the structure of nanorods with 200–1000 nm in length and 50–100 nm in width. The results clearly exhibited that the structure of nanorods was successfully synthesized during the MCM. Moreover, some plate-like nanocatalysts can be observed in Fig. 4a. Furthermore, the active phases containing potassium components were uniformly dispersed on the surface of a support, which have particle size between 10 and 25 nm.

The KCA/C nanocomposite showed worm-like structure that can be related to lack of combustion heat for growth of $Ca_{12}Al_{14}O_{33}$ to form nanorods. However, it was clearly observed that the porosity of the KCA/C nanocomposite was much more than that of the KCA nanocatalyst. The KCA/C nanocomposite showed highly porous structure, which was formed by huge volume of gases exhausted during the decomposition of dextrose as fuel [33]. These porosities can significantly affect the activity of the samples in the MTR.

The EDX analyses of the KCA and KCA/C samples are shown in Fig. 5. Both the samples showed no impurity in their structures and the KCA sample did not show any carbon element in its structure. It can be seen that the EDX compositions of the as-synthesized KCA catalyst were close to its nominal values. Moreover, the KCA/C sample contained a high amount of carbon groups that can increase its ability to absorb microwave irradiation. Dot-mapping analysis of both the samples showed well dispersion of elements where no agglomeration was observed on the surface of the samples. The reason could be that the MCM is a sufficient method for fabricating nanocatalysts with well crystallinity and well distribution of active phases on the support without any agglomeration.

3.5. BET–BJH analysis

The N_2 adsorption–desorption isotherms of KCA and KCA/C are illustrated in Fig. S2 (SM). The samples exhibited type IV isotherms as defined by the IUPAC classification.
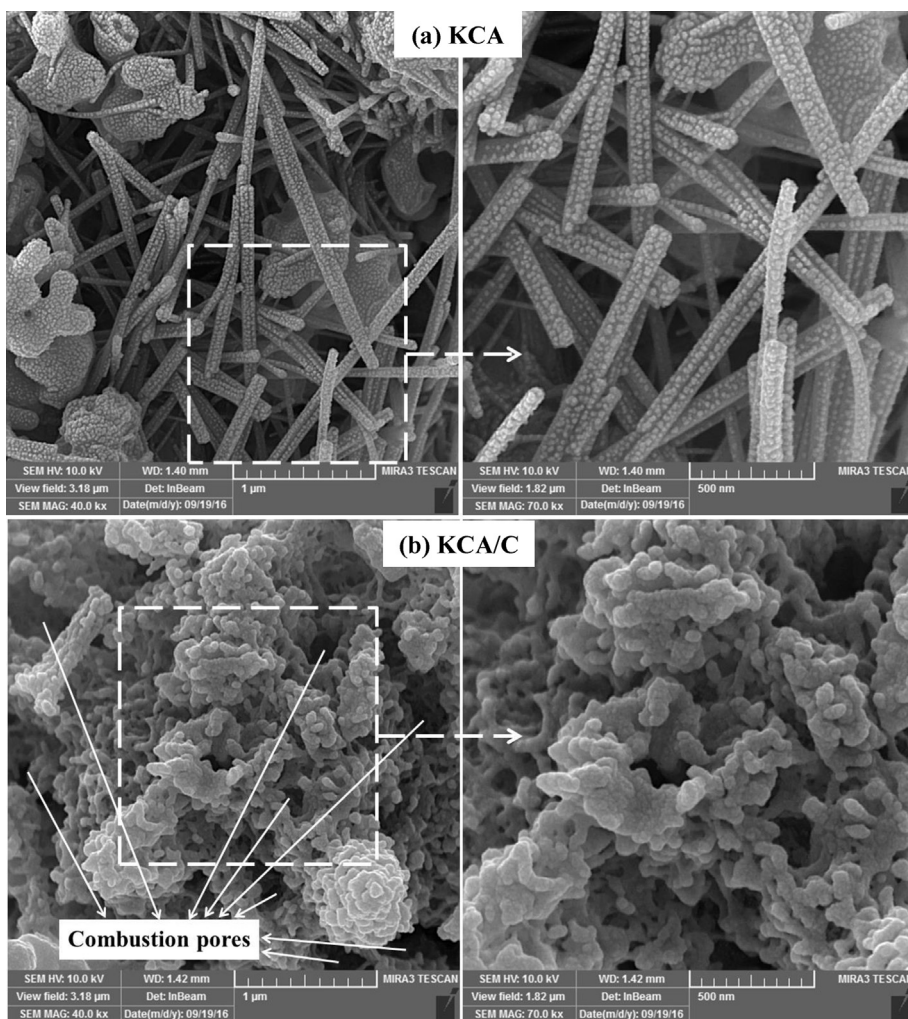
Fig. 4. FESEM images of (a) KOH/Ca$_{12}$Al$_{14}$O$_{33}$ and (b) carbonated KOH/Ca$_{12}$Al$_{14}$O$_{33}$ nanocatalysts.

The hysteresis loops expected for this case were of H3 type that confirmed the plate-like particles, advance to the slit-shaped pores [4]. The BET surface area, total pore volume, and mean pore size of KCA significantly increased when dextrose as fuel was used instead of urea to form the KCA/C nanocomposite. The textural properties increased from 131.65 to 152.22 m^2/g, from 0.382 to 0.546 mL/g, and from 74.2 to 79.6 Å, respectively. This could be due to the formation of a large molecule of carbon groups that meaningfully affected the surface area and pore volume.

3.6. Activity analysis

The activity of the KCA and KCA/C nanocomposites was assessed at various microwave powers (180, 270, 360, 450, and 540 W) as depicted in Fig. 6. The FAME content obtained by the KCA nanocatalyst increased from 25.1% to 97.5% with increase in microwave power from 180 to 360 W; then, the content was maintained constant and finally decreased to 90.4% at 540 W microwave power. Similar behavior was seen in the KCA/C nanocomposite

where microwave power of 270 W was selected as an optimum amount to achieve high conversion. Methanol and KCA/C nanocomposite as microwave absorber materials can absorb higher amount of microwave irradiation by increasing the microwave power. Therefore, the FAME content of produced biodiesel would be raised. In addition, microwave irradiation accelerated the reaction rate and increased the conversion of canola oil to biodiesel after short time. Therefore, the reaction using KCA/C as a nanocatalyst rapidly increased because of more absorption of microwave irradiation by this reaction medium.

The reduction in the conversion of canola oil to biodiesel at higher microwave power can be attributed to evaporation of a high amount of methanol and reduction of methanol in the reaction medium. Comparing the catalytic activity of the two nanocatalysts exhibited that the catalytic activity of KOH/Ca$_{12}$Al$_{14}$O$_{33}$ sharply increased when it was loaded with carbon groups such that the higher FAME content was obtained at lower microwave power. It can be concluded that the carbon groups in the nanocatalyst structure acted as a microwave absorber.
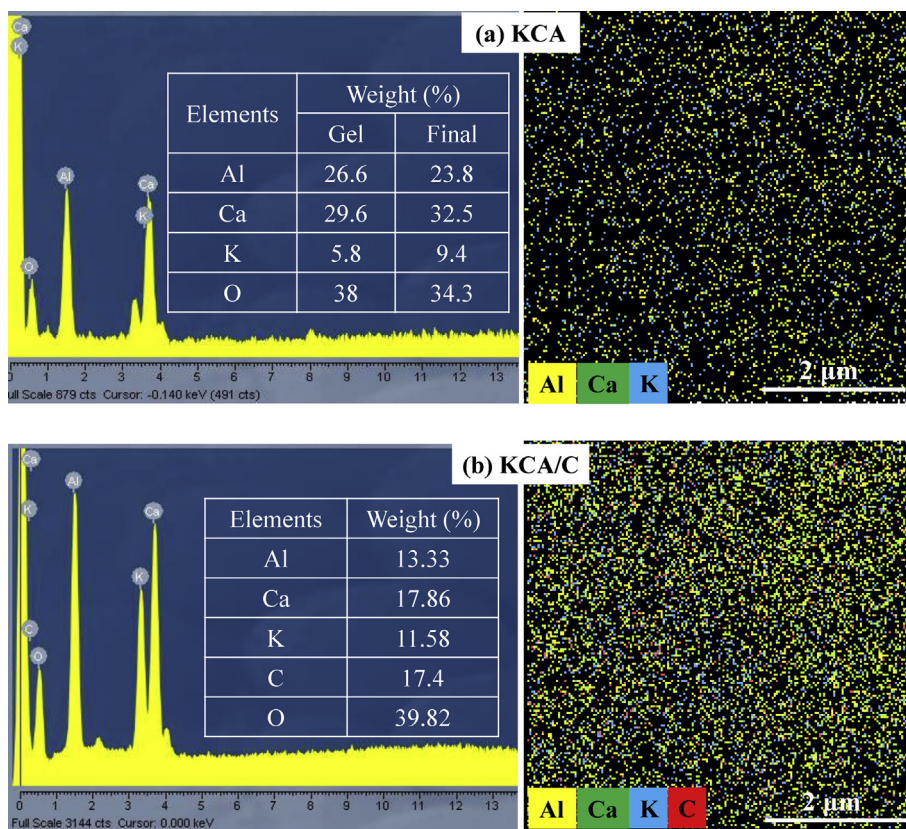
Fig. 5. EDX analysis of (a) $KOH/Ca_{12}Al_{14}O_{33}$ and (b) carbonated $KOH/Ca_{12}Al_{14}O_{33}$ nanocatalysts.
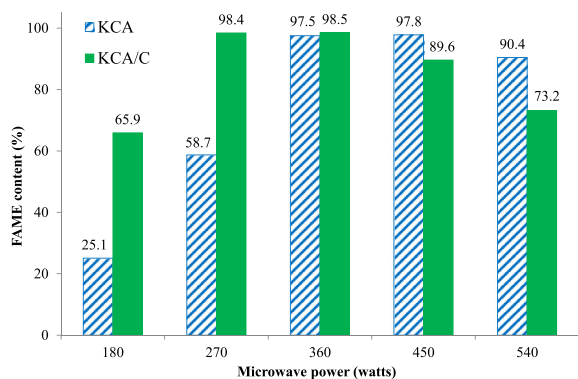
Fig. 6. Catalytic activity of $KOH/Ca_{12}Al_{14}O_{33}$ and carbonated $KOH/Ca_{12}Al_{14}O_{33}$ nanocatalysts in the MTR. Reaction conditions: methanol/oil molar ratio of 18, 4 wt% of the catalyst, and 45 min of reaction time.

The basicity of the samples determined by titration with 0.02 M benzoic acid solution in ethanol using Hammett indicators exhibited that the basic strength of both the samples was between 9.8 and 15 with total basicity of 0.518 and 0.542 mmol/g corresponding to KCA and KCA/C, respectively. Although the basicity had a significant effect on the catalytic activity, the conversion of canola oil was very much higher using KCA/C than using KCA (around two times at microwave power of 180 and 270 W), which

cannot be only related to basicity. Therefore, the carbon groups extremely increased the activity of the samples for the MTR, which was definitely related to their ability to absorb microwave irradiation.

3.7. Optimization of microwave-assisted biodiesel production conditions

3.7.1. Effect of catalyst concentration

The effect of the catalyst amount on the conversion of canola oil to biodiesel under microwave irradiation is illustrated in Fig. S3. The reaction was performed under the conditions of 270 W microwave power, methanol/oil molar ratio of 18, and 45 min of reaction time. The results presented that the conversion increased from 81.4% to 98.4% when the catalyst concentration increased from 2 to 4 wt%, which is related to an increase in the available active surface area for reactants [34]. Because of more absorption of microwave irradiation and evaporation of methanol to vapor phase, the conversion decreased with more loading of the KCA/C nanocomposite. Therefore, 4 wt% of the catalyst was chosen as optimum.

3.7.2. Effect of methanol/oil ratio

Methanol amount has an important role in achieving high conversion in the transesterification reaction where the reaction goes in the forward direction with a high

amount of methanol. Moreover, methanol is a polar component that can absorb the microwave irradiation to accelerate the reaction. As shown in Fig. S4, the conversion dramatically increased from 71.9% to 97.9% with an increase in the methanol/oil molar ratio from 9 to 15 and then slightly increased to 98.4%. The reduction in the activity with the methanol/oil molar ratio of 21 can be attributed to a high amount of microwave absorption, which caused evaporation of the high amount of methanol, and/or fouling of the porosity of nanocatalysts with methanol, which reduced the available active surface area of the catalyst [35].

3.7.3. Effect of reaction time

Influence of reaction time in the MTR was assessed under the conditions of 270 W microwave power, methanol/oil molar ratio of 15, and 4 wt% of the catalyst. The results are presented in Fig. S5. The conversion was, respectively, obtained as 45.4%, 91.6%, 98.8%, and 97.9% for the reaction time of 10, 20, 30, and 45 min. With an increase in the reaction time, the reactants had enough time to react with each other to form biodiesel and reach to equilibrium point. Therefore, the reaction time was set at 30 min.

The composition of the produced biodiesel at the optimized conditions is presented in Fig. 7. It was observed that methyl oleate was the main composition of the produced biodiesel (58.1%) and canola oil biodiesel mainly contained unsaturated methyl esters (89.4%) that had negative effect on oxidation stability of the biodiesel.

3.8. Reusability

The reusability of the KCA/C nanocomposite, as an important factor for industrial application of a catalyst, was evaluated in the MTR at optimum conditions. When the catalyst was separated from the reaction mixture after each reaction, the catalyst was washed twice with hexane and calcined at 800 °C for 1 h under ambient argon. As shown in

Fig. 8, the KCA/C nanocomposite preserved its activity for at least four times (conversion over 90%). The less reduction in the activity can be due to leaching and/or poisoning of potassium components as active phases. The results demonstrated that because of the simple preparation method for the synthesis of the carbonated KOH/mayenite nanocomposite with high activity and stability, it had high ability for industrial application in the MTR process.

3.9. Biodiesel properties

The properties of the biodiesel produced from canola oil are listed in Table 1. The biodiesel showed an appropriate ester content (>96.5%). Other properties such as density, viscosity, cloud point, pour point, flash point, and acid value had a good agreement with the standard values (EN 14214 and ASTM D-6751). The results confirmed that the KCA/C nanocomposite was an attractive nanocatalyst for
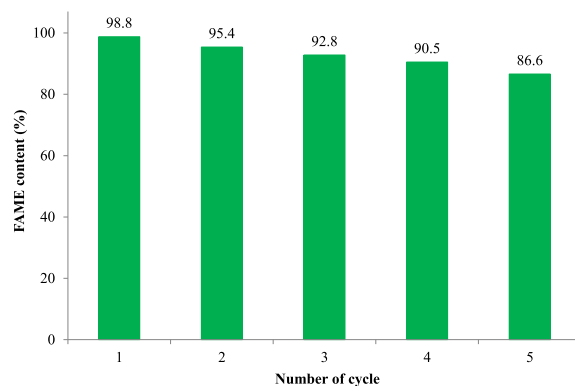
Fig. 8. Reusability of a carbonated $KOH/Ca_{12}Al_{14}O_{33}$ nanocomposite for biodiesel production under microwave irradiation. Reaction conditions: microwave power of 270 W, methanol/oil molar ratio of 15, 4 wt% of the nanocatalyst, and 30 min of reaction time.
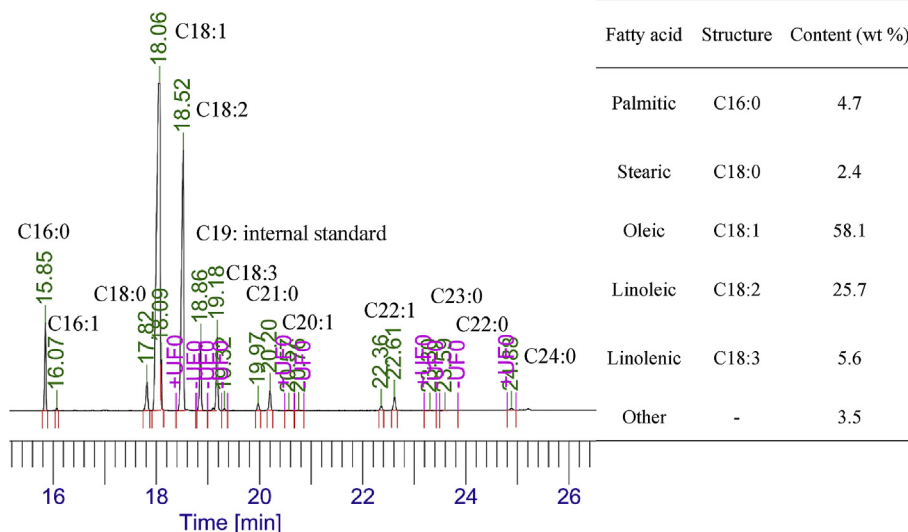
Fatty acid	Structure	Content (wt %)
Palmitic	C16:0	4.7
Stearic	C18:0	2.4
Oleic	C18:1	58.1
Linoleic	C18:2	25.7
Linolenic	C18:3	5.6
Other	-	3.5

Fig. 7. Composition of FAMEs of produced biodiesel at optimum conditions.

Table 1
Properties of canola biodiesel obtained by the MTR using a carbonated $KOH/Ca_{12}Al_{14}O_{33}$ nanocomposite.

Property	Unit	ASTM D-6751 standard	EN 14214 standard	Biodiesel value
Ester content	(w/w)%	96.5<	96.5<	98.8
Density	g cm^{-3}	800–900	860–900	876
Viscosity (40 °C)	mm^2 s	1.9–6	3.5–5	4.53
Flash point	°C	130<	120<	159
Pure point	°C	–	–	−9
Cloud point	°C	–	–	−1
Acid value	mg KOH/g	<0.5	<0.5	0.22

industrial biodiesel production in accordance with the standard specification.

4. Conclusions

Effect of loading of carbon groups on the activity of the $KOH/Ca_{12}Al_{14}O_{33}$ nanocatalyst for absorption of microwave irradiation to accelerate the MTR was evaluated. For this purpose, the carbon-supported $KOH/Ca_{12}Al_{14}O_{33}$ nanocomposite was synthesized by the MCM via dextrose as a carbon source. The results showed that the as-synthesized KCA/C nanocomposite could convert a higher amount of canola oil to biodiesel under the MTR as compared to the KCA nanocatalyst, due to its large pore size, surface area, and ability for absorption of microwave irradiation. Under the optimum conditions of the MTR (270 W microwave power, methanol/oil molar ratio of 15, 4 wt% of the nanocomposite, and 30 min of reaction time), the KCA/C nanocomposite exhibited high stability for several uses. Furthermore, the density, kinematic viscosity at 40 °C, acid number, pure point, cloud point, and flash point of the as-produced biodiesel were characterized and showed good agreement with the standard value of EN 14214 and ASTM D-6751.

Acknowledgments

Appendix A. Supplementary data

Supplementary data related to this article can be found at https://doi.org/10.1016/j.crci.2018.04.003.

References

[1] I. Bilecka, M. Niederberger, Nanoscale 2 (2010) 1358.
[2] C.O. Kappe, Chem. Soc. Rev. 37 (2008) 1127.
[3] R. Liu, X. Wang, X. Zhao, P. Feng, Carbon 46 (2008) 1664.
[4] M. Hashemzehi, N. Saghatoleslami, H. Nayebzadeh, C. R. Chimie 19 (2016) 955.
[5] C.-C. Liao, T.-W. Chung, Chem. Eng. Res. Des. 91 (2013) 2457.
[6] W. Ye, Y. Gao, H. Ding, M. Liu, S. Liu, X. Han, J. Qi, Fuel 180 (2016) 574.
[7] M.-C. Hsiao, C.-C. Lin, Y.-H. Chang, Fuel 90 (2011) 1963.
[8] K.-S. Chen, Y.-C. Lin, K.-H. Hsu, H.-K. Wang, Energy 38 (2012) 151.
[9] Y.-C. Lin, S.-C. Chen, C.-E. Chen, P.-M. Yang, S.-R. Jhang, Fuel 135 (2014) 435.
[10] W. Liu, P. Yin, X. Liu, W. Chen, H. Chen, C. Liu, R. Qu, Q. Xu, Energy Convers. Manag. 76 (2013) 1009.
[11] S. Zhang, Y.-G. Zu, Y.-J. Fu, M. Luo, D.-Y. Zhang, T. Efferth, Bioresour. Technol. 101 (2010) 931.
[12] D. Kim, J. Choi, G.-J. Kim, S.K. Seol, Y.-C. Ha, M. Vijayan, S. Jung, B.H. Kim, G.D. Lee, S.S. Park, Bioresour. Technol. 102 (2011) 3639.
[13] M.R. Quirino, M.J.C. Oliveira, D. Keyson, G.L. Lucena, J.B.L. Oliveira, L. Gama, Mater. Res. Bull. 74 (2016) 124.
[14] B.R. Vahid, M. Haghighi, Energy Convers. Manag. 126 (2016) 362.
[15] M. Sharma, A.A. Khan, K.C. Dohhen, J. Christopher, S.K. Puri, D.K. Tuli, R. Sarin, J. Am. Oil Chem. Soc. 89 (2012) 1545.
[16] G. Tao, Z. Hua, Z. Gao, Y. Chen, L. Wang, Q. He, H. Chen, J. Shi, RSC Adv. 2 (2012) 12337.
[17] H. Nayebzadeh, N. Saghatoleslami, M. Tabasizadeh, J. Taiwan Inst. Chem. Eng. 68 (2016) 379.
[18] H. Yuan, B.L. Yang, G.L. Zhu, Energy Fuel. 23 (2008) 548.
[19] Y. Zhou, S. Niu, J. Li, Energy Convers. Manag. 114 (2016) 188.
[20] B. Ye, F. Qiu, C. Sun, Y. Li, D. Yang, J. Chem. Technol. Biotechnol. 89 (2014) 988.
[21] J.P. da Costa Evangelista, A.D. Gondim, L.D. Souza, A.S. Araujo, Renew. Sustain. Energy Rev. 59 (2016) 887.
[22] G. Postole, T.-S. Nguyen, M. Aouine, P. Gélin, L. Cardenas, L. Piccolo, Appl. Catal. B Environ. 166–167 (2015) 580.
[23] P. Kumar, V.C. Srivastava, I.M. Mishra, Kor. J. Chem. Eng. 32 (2015) 1774.
[24] R. Ianos, C. Păcurariu, G. Mihoc, Ceram. Int. 40 (2014) 13649.
[25] H. Takehara, M. Fujiwara, M. Arikawa, M.D. Diener, J.M. Alford, Carbon 43 (2005) 311.
[26] C. Zhu, C.-G. Han, G. Saito, T. Akiyama, J. Alloy. Comp. 689 (2016) 931.
[27] S. Lu, H. Chunfeng, S. Yoshio, H. Qing, J. Phys. Appl. Phys. 45 (2012) 215302.
[28] Y.-P. Chang, P.-H. Chang, Y.-T. Lee, T.-J. Lee, Y.-H. Lai, S.-Y. Chen, Microporous Mesoporous Mater. 183 (2014) 134.
[29] S.N. Titova, G.A. Domrachev, S.Y. Khorshev, A.M. Ob'edkov, L.V. Kalakutskaya, S.Y. Ketkov, V.K. Cherkasov, B.S. Kaverin, K.B. Zhogova, M.A. Lopatin, V.L. Karnatsevich, E.A. Gorina, Phys. Solid State 46 (2004) 1365.
[30] L. Stobinski, B. Lesiak, L. Kövér, J. Tóth, S. Biniak, G. Trykowski, J. Judek, J. Alloy. Comp. 501 (2010) 77.
[31] V.I. Srdanov, A.P. Saab, D. Margolese, E. Poolman, K.C. Khemani, A. Koch, F. Wudl, B. Kirtman, G.D. Stucky, Chem. Phys. Lett. 192 (1992) 243.
[32] S. Iglesias-Groth, F. Cataldo, A. Manchado, Mon. Not. Roy. Astron. Soc. 413 (2011) 213.
[33] G. Saito, C. Zhu, C.-G. Han, N. Sakaguchi, T. Akiyama, Adv. Powder Technol. 27 (2016) 1730.
[34] H. Nayebzadeh, N. Saghatoleslami, A. Maskooki, B. Rahmani Vahid, Chem. Biochem. Eng. Q. 25 (2014) 259.
[35] K. Srilatha, N. Lingaiah, B.L.A.P. Devi, R.B.N. Prasad, S. Venkateswar, P.S.S. Prasad, Appl. Catal. Gen. 365 (2009) 28.